Indian Journal of Fibre& Textile Research
Vol. 50, September 2025, pp. 292-302
DOI: 10.56042/ijftr.v50i3.10434

Effect of GO/rGO coating on morphological, thermal, and mechanical properties of sisal fibres

Jitendra Kumar Gautam[1,a] & Rabindra Kumar Patel[2]

[1]Uttar Pradesh Textile Technology Institute, Kanpur 208 001, India

[2]Department of Mechanical Engineering, Motilal Nehru National Institute of Technology, Allahabad, 211 004, India

Received 16 April 2024; revised received and accepted 24 October 2024

This study investigates the potential of natural lignocellulose fibres (NLFs) as sustainable alternatives to synthetic fibres by addressing their inherent limitations in mechanical, interfacial, and thermal performance. Sisal fibres have been subjected to 5 wt% alkali treatment followed by coating with 1 wt% graphene oxide (GO) and reduced graphene oxide (rGO). Structural and thermal characterizations have been carried out using Fourier transform infrared spectroscopy (FTIR), X-ray diffraction (XRD), and thermogravimetric analysis (TGA). The presence of GO/rGO coating has been confirmed by FTIR, while XRD analysis has revealed improved crystallinity. Mechanical testing has demonstrated significant enhancements in tensile strength by approximately 62% (GO) and 94% (rGO), along with increases in interfacial shear strength by nearly 95% and 133%, respectively, compared with untreated fibres. These findings have shown that GO/rGO-coated sisal fibres exhibit superior performance while maintaining environmental compatibility, making them promising candidates for applications in automotive, aerospace, household products, sports, and naval vessel industries.

Keywords: GO and rGO coating, Interfacial shear strength, Morphology, Sisal fibres, Tensile strength

1 Introduction

Plastic is becoming popular in various industrial and widespread applications due to its excellent characteristics. However, despite their convenience in our lives, they have also given rise to numerous challenges. Most plastics are non-biodegradable, and burning them releases many hazardous chemicals, contributing to "white pollution" throughout the planet[1]. Instead of plastic, some fossil fuels like petroleum have been designated as the primary global source of greenhouse gases like carbon dioxide. Industries and researchers have focused on ecology and sustainable development issues for the last few years to overcome these problems. Even though petroleum-derived polymeric materials are still used in various applications, including the automotive, civil construction, and packaging industries, these sectors are the biggest waste producers. The use of fibres and resins is tremendously increasing in these sectors. To fulfil the demand of the above industries, natural fibres can be used as a substitute for non-renewable materials and satisfy the need for eco-friendly products[2].

Due to their lower environmental effect, NLFs (natural lignocellulosic fibres) are becoming increasingly popular among composites makers and material scientists. These are becoming popular due to their properties like biodegradability, low cost, affordability, good mechanical qualities, low density, and simplicity of construction. Additionally, these fibres provide benefits, including reduced wear and tear and corrosion resistance. Polymer-based matrices use NLFs (flax, jute, sisal, hemp, and kenaf) as reinforcement materials. Most industries seek NLFs because of economic and social awareness and the high cost of petroleum products. Lightweight natural fibres like sisal, flax, jute, kenaf, and hemp might easily replace many synthetic fibres and mineral fillers in several applications like sports goods, automotive, textile, and aerospace industries[3]. Natural fibres can be used as viable replacements for synthetic fibres to strengthen the polymer matrix due to their low density, low cost, availability in abundance, high specific strength, and modulus[3]. Comparing the properties of glass fibres reinforced with a polymer matrix and other synthetic fibres,[4] previous publications have already revealed a superior result: Jute, flax, sisal, piassava, and kenaf are just a few of the NFLs that have already been researched for engineering purposes[2].

[a]Corresponding author.
E-mail: jitendra.uptti@gmail.com

Among the various NLFs, sisal fibre is among the most popular due to its excellent characteristics. It is one type of fibre taken from agave-family plants' leaves. When scraped from newly cut plant leaves, the sisal fibre is stiffer, more robust, and less flexible. Sisal fibre is produced in Africa, including Kenya, Tanzania, and Madagascar; South America, such as Venezuela and Brazil; Southern Mexico; and China, with Brazil and Tanzania being particularly significant producers. Other smaller producers include Cuba, Indonesia, and Haiti[5]. It has excellent specific strength, durability, ability to stretch, and resistance to saltwater damage[2].

Conversely, the NFLs have significant drawbacks compared to synthetic materials, including a high moisture absorption and hydrophilic surface; these make it challenging to utilise them as reinforcing materials in composites[2]. Weak bonds form between polymers and the surface of NFLs due to the hydrophobic character of polymers and the hydrophilic nature of NFLs. A reduction in mechanical performance may happen due to dimensional changes, such as swelling, induced by the moisture absorption tendency of fibres[2]. Sisal fibres also possess hydrophilic characteristics because of their highly polarised hydroxyl groups[6]. Its contaminants, such as wax and natural oils, are the main issue. Its inability to be used as reinforcement in polymer composites is critically hampered by poor bonding between the non-polar hydrophobic matrix and the polar hydrophilic fibre. Therefore, changes to the fibre surface qualities are being made by using various chemical treatments. Several attempts have been made to increase the interfacial adhesion between natural fibres and polymer matrix[7]. These chemical treatments primarily reduce their surface polarity to improve the natural fibres' interfacial adhesion with the polymer matrix. Alkali treatment is a widely used and cost-effective procedure that effectively alters the surface of NLF, enhancing its mechanical characteristics. When first extracted from plants, NLFs consist of microfibril bundles bound to amorphous substances, including lignin, hemicellulose, and waxes[8]. Alkali treatment removes the natural binder of fibres, so microfibrils are reorganised in the direction of tensile loading. The alkali treatment also induces a more textured surface, facilitating enhanced adhesion between fibre and matrix, enhancing the composite's performance[8]. Sisal fibre that has been alkali-treated loses noncellulosic components, primarily hemicellulose and some lignin[9]. The sisal fibre's interfibrillary area contains hemicelluloses. The fundamental cause of the production and release of stress in stretched sisal fibre is the distortion of this fibrillary network.

In addition to alkali treatment, other researchers have conducted different chemical treatments to improve the mechanical properties of sisal fibres. During their investigation, Chand *et al.*[10] discovered that the mechanical properties of sisal fibre are enhanced by the coating of various polymers, including polyvinyl alcohol, polypropylene, polyester, polystyrene (PS), polyvinyl alcohol and araldite epoxy. The composite was fabricated by Hakim *et al.*[11] using polystyrene-coated sisal fibres and HDPE. The composite underwent mechanical and water absorption tests, revealing enhanced mechanical properties and reduced water absorption. Hu *et al.*[12] utilised the ultrasonic impregnation method for alkali/polyvinyl coating and observed enhanced mechanical properties. Sahu and Gupta[13] conducted a study on using an eco-friendly polymer, specifically PLA, on sisal fibres. They produced a composite material and conducted mechanical and thermal tests to analyse its properties. Behra *et al.*[14] investigated the thermal, mechanical and tribological properties of sisal fibres by the use of Sodium citrate (SC) and stearic acid (SA). Jena *et al.*[15] investigated untreated, chemically treated, and emulsion-coated sisal fibres' mechanical, physical, elemental, morphological, and crystallographic properties.

Since its discovery in 2004, graphene material with a just one-atom-thick structure has garnered much attention due to its remarkable features. These properties include mechanical strength and electrical conductivity. "Graphene oxide (GO) is one kind of graphene derivative, consisting of a flat layer of sp2-bonded carbon atoms with many oxygen functional groups grafted on the surface"[16]. The GO membranes, consisting of stacked GO sheets, exhibit impermeability to gases, vapours, and liquids[2]. Using GO to functionalise natural fibres in composite materials enhances their mechanical and thermal characteristics by increasing the fibre's interfacial adhesion with a polymer matrix[17].

The application of graphene oxide (GO) in the surface treatment of NLFs is gaining attention among researchers as a promising alternative. This is primarily due to its ability to form interfacial solid interactions with reactive areas and its biocompatibility[18]. This study aims to assess sisal fibres' mechanical, chemical and thermal

characteristics that have been functionalised with GO/rGO and treated with mercerisation.

Sarker *et al.*[19] (2018) conducted an investigation into the coating of graphene oxide (GO) and graphene flaxes (G) onto jute fibres. They discovered that the interfacial shear strength was increased by approximately 236 % and the tensile strength by approximately 96 % compared to untreated fibres. This was achieved by establishing either bonding (GO) or mechanical interlocking (G) between the fibres and graphene-based flakes. Hallad *et al.*[20] conducted an investigation into the formation of a nano composite by combining nano graphene with hemp fibres and L-12 epoxy resin, and observed enhanced properties. Costa *et al.*[21] investigated a graphene oxide-coated curaua fibre reinforced epoxy composite for multilayered ballistic armour application. Filho *et al.*[22] investigated the thermal behaviour of graphene oxide-coated piassava fibre and its composite and found improved thermal stability. Silveira *et al.*[23] examined the thermal and chemical properties of hemp fibres having graphene oxide coating and alkali treatment. Sarker *et al.*[24] investigated nanoengineered graphene-based jute fibre composites and discovered that their Young's modulus and tensile strength were enhanced by approximately 324 % and 110 %, respectively. Various researchers have applied graphene material coatings to various natural fibres, and their effects have been examined. This research endeavours to determine sisal fibres' morphology, thermal, and mechanical properties by coating them with graphene oxide and reduced graphene oxide.

2 Materials and Methods

2.1 Sisal Fibres

Sisal fibres were purchased from Vruksha Composites, Guntur, Andhra Pradesh, India. Their chemical composition and mechanical properties are listed in Table 1.

Table 1 — Properties and chemical composition of sisal fibre[25]

Properties	Value
Density, g/m^3	1.45
Tensile strength, MPa	126-860
Tensile modulus, GPa	7-13
Elongation at break, %	1.54-3.85
Cellulose, %	65-78
Hemicellulose, %	10-14
Wax, %	2
Pectin, %	10.1
Lignin, %	9.9
Moisture content, %	10
Ash, %	0.6-1

2.2 Graphene Material

Graphene oxide (GO), a graphene derivative rich in oxygen-containing functional groups such as hydroxyl, carboxyl, carbonyl, and epoxy moieties, was purchased from Adnano Technologies, Industrial Area Road, Machenahalli, Karnataka, India. he GO supplied was synthesised using a modified Hummers' method and exhibited high surface area and hydrophilicity.

Reduced graphene oxide (rGO), obtained by chemical or thermal reduction of GO to decrease oxygen content, was also procured from Adnano Technologies. The properties of GO and rGO are given in Table 2.

2.3 Alkaline Treatment

Alkaline treatment of sisal fibres was performed using sodium hydroxide (NaOH) pellets (Merck, India). A 5 wt% NaOH solution was prepared at a material-to-liquor ratio of 1:50. Approximately 10 g of sisal fibres were immersed in the solution for 1 h to remove hemicelluloses. The treated fibres were then thoroughly rinsed under running water 8–10 times until neutral pH was attained, followed by drying in a hot-air oven at 80 °C for 12 h. Fig. 1 depicts the sisal fibres and treatment process.

2.4 GO and rGO Coating on Sisal Fibres

GO and rGO dispersions (1 wt %) were prepared in deionised water for coating. The alkali-treated fibres were immersed in these solutions using a dip-coating method at a material-to-liquor ratio of 1:10. After immersion, fibres were dried at 80 °C for 3 h. The nomenclature used for the specimens is provided in Table 3.

2.5 Characterisation

2.5.1 Thermogravimetric Analysis (TGA)

Thermal stability of fibres was examined using a Perkin Elmer TGA 4000 in a nitrogen atmosphere. The samples were heated from 30 °C to 700 °C at a rate of 10 °C/min. Fibres were pre-dried, cut into small fragments, and placed in a platinum crucible for testing.

Table 2 — Properties of graphene oxide and reduced graphene oxide[24]

Properties	GO	rGO
Thickness, Z	~0.8-2 nm	~0.8-2 nm
Dimension, X & Y	~5-10 µm	~5-10 µm
Number of layers	1-3	1-3
Oxygen content	~30 %	~5 %
Surface area	~120 m^2/g	~400 m^2/g
Bulk density	0.8-1 g/cm^3	0.014 g/cm^3

Fig. 1 — Morphological images showing (a) Untreated sisal fibres, (b) graphene oxide, (c) reduce graphene oxide, (d) sisal fibres after combing, (e) sisal fibres immersed in NaOH solution, (f) GO-coated sisal fibres and (g) rGO-coated sisal fibres

Table 3 — Nomenclature adopted for specimens

Nomenclature	Specimen
SF	Sisal fibre
SF+AT	5 wt % alkali-treated sisal fibre
SF+AT+GO	5 wt % alkali-treated 1.0 wt % GO-coated sisal fibre
SF+AT+rGO	5 wt % alkali-treated 1.0 wt % rGO-coated sisal fibre

2.5.2 ATR-FTIR Spectroscopy

Chemical interactions and bonding changes in fibres were analysed using a Bruker ALPHA spectrometer equipped with ATR mode. Spectra were collected in the range of 500–4000 cm^{-1} with a resolution of 4 cm^{-1}.

2.5.3 X-Ray Diffraction (XRD)

Crystallinity of fibres was determined using a PROTO AXRD diffractometer with Cu Kα radiation (λ = 1.54 Å), operated at 30 kV and 20 mA. The diffraction patterns were recorded in the 2θ range of 10–60° with a scanning speed of 0.02°/s. Crystallinity (%) and crystallinity index (C.I.) were calculated using Eqs. (1) and (2) [26].

$$\% \, Cr = \frac{I_{002}}{I_{002}+I_{am}} \quad ...(1)$$

$$C.I = \frac{I_{002}-I_{am}}{I_{002}} \quad ...(2)$$

where 'I_{002}' shows the maximum intensity of crystalline at 2θ = 21.46-22.02°; and 'I_{am}', intensity of the amorphous material at 2θ = 18.32-18.48°.

2.5.4 Scanning Electron Microscopy (SEM)

Surface morphology of untreated, alkali-treated, and GO/rGO-coated fibres was observed using a JEOL JCM-7000 scanning electron microscope at 10 kV with magnifications of 500 x to 1000 x. Fibres were cut and fixed on double-sided carbon tape. A skinny layer of gold plating was applied to the fibres in the DII-29030SCTR Smart Coater apparatus.

2.5.5 Tensile Testing of Elementary Fibres

Alkali-treated and coated fibres were fibrillated using a comb and separated into elementary fibres. Each fibre was mounted on a paper frame with cyanoacrylate adhesive and conditioned for 24 h at 20 ± 2 °C and 55% RH. Fibre diameters were measured at five random points using a digital microscope. Tensile properties were tested using an Instron-3366 universal testing machine in accordance with ASTM D3822-01, with a gauge length of 20 mm and crosshead speed of 2 mm/min. Modulus was determined from the slope of the stress–strain curve in the 0.1–0.3% strain region.

2.5.6 Single-Fibre Microbond Test

For the individual fibre microbond test, all primary fibres were manually separated and cut to a length between 30 and 50 mm. Next, primary fibres were superglued to a 25 × 10 mm window of paper card frame with very little strain. Small epoxy resin (Araldite LY556) droplets were applied to fibres and cured for 24 h. Droplet dimensions were measured using a Keyence digital microscope (WESWOX- TRHL-66A) (125×). Tests were conducted on an Instron-3366 using a rotating microvise equipped with sharp blade edges[27], at a loading rate of 0.2 mm/min. Interfacial shear strength (IFSS) was calculated using Eq. 3:

$$\tau_{IFSS} = \frac{F}{\pi D l_e} \quad \ldots (3)$$

where F is the maximum load; D, the fibre diameter; and l_e, embedded length of the microdroplet[19]. Data from 50 samples were averaged to obtain IFSS values.

2.6 Statistical Analysis

To analyse the tensile failure behaviour and the failure occurring at the fibre/matrix interface, Weibull statistical analysis was employed. The cumulative

probability of failure[19] was determined using the following equation:

$$P = 1 - \exp\left(\left(\frac{\sigma_t}{\sigma_0}\right)^m\right) \quad \ldots (4)$$

where m is the Weibull shape parameter; σ_t, tensile strength; and σ_o, Weibull scale parameter.

By taking the double natural logarithm of Eq. (4), the following linearised form is obtained:

$$\ln(-\ln(1-P)) = m(ln\ \sigma_t - ln\ \sigma_0) \quad \ldots (5)$$

For fibre/matrix interaction, σ_t (tensile strength) was replaced with τ_s (shear strength) to evaluate the failure behaviour under shear loading conditions.

3 Results and Discussion

3.1 TGA (Thermogravimetric Analysis)

The thermogravimetric analysis (TGA) of untreated and graphene material-coated sisal fibres reveals weight loss patterns associated with the decomposition of cellulose, hemicellulose, and lignin. These constituents significantly influence the thermal stability of fibres. The TGA curves (Fig. 2) demonstrate degradation in three distinct phases: 100–250 °C, 250–380 °C, and 380–700 °C, corresponding to the decomposition of hemicellulose, cellulose, and lignin, respectively. Among these, lignin degrades most slowly[27]. Table 4 shows that alkali-treated sisal fibres undergo less weight loss compared to untreated fibres. This behaviour is attributed to the partial removal of hemicellulose, which enhances thermal stability[28]. As sisal fibres are naturally hydrophilic, the removal of hemicellulose by alkali treatment reduces their water absorption capacity, thereby limiting thermal degradation.

Fibres coated with GO and rGO exhibit the least weight loss, indicating improved thermal stability. In the first degradation stage (100–250 °C), weight loss ranges from 5.48–10.59 % due to the elimination of moisture. The second stage (250–380 °C) corresponds to hemicellulose decomposition. Thermal breakdown occurs at 441.98 °C for untreated fibres, 474.8 °C for alkali-treated fibres, 528.77 °C for GO-coated fibres, and 569.23 °C for rGO-coated fibres. These results confirm that graphene-based coatings act as a protective barrier, delaying decomposition[24]. The breakdown of the proto-lignin bond causes deterioration over 400 °C[32]. At 25 % mass loss, the thermal stability of GO- and rGO-coated fibres increases by 12–14 °C compared to untreated fibres.

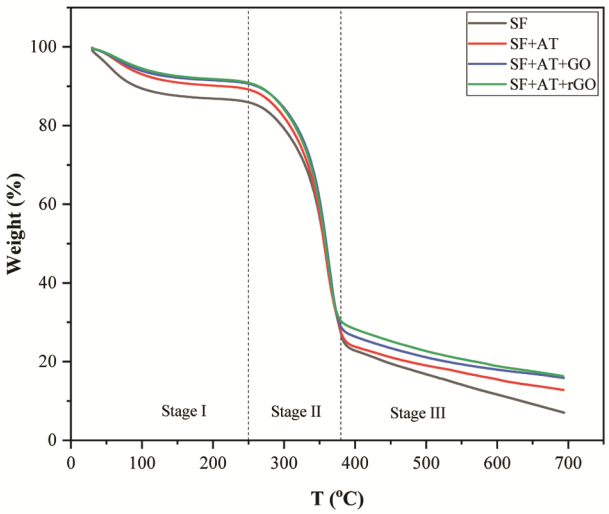

Fig. 2 — TGA graph of untreated, alkali-treated, GO-coated, and rGO-coated sisal fibres

Table 4 — Weight loss to temperature

Temperature, °C	SF	SF+AT	SF+AT +GO	SF+AT +rGO
100	10.59	6.97	6.12	5.88
200	13.14	9.84	8.48	8.16
300	20.75	17.90	15.53	15.86
400	77.21	76.19	73.66	71.72
500	82.95	80.97	78.91	77.32
600	88.38	85.46	82.03	81.12

Developing a carbonaceous barrier of GO and rGO on the surface of fibres slows the deterioration and enhances the fibre's thermal stability[29]. The SF+AT+rGO fibres demonstrate the lowest weight loss in the final stage of deterioration, signifying superior thermal stability compared to untreated (SF), alkali-treated (SF+AT), and GO-coated (SF+AT+GO) fibres. This enhancement is due to the formation of a carbonaceous barrier on the fibre surface, which slows degradation and enhances overall stability.

3.2 X-Ray Diffraction (XRD)

The crystallographic structures of neat, alkali-treated, and GO/rGO-coated sisal fibres are investigated using XRD (Fig. 3). CuKα (λ = 1.54) radiation with 2θ angle from 10° and 60° were used for XRD analysis. The three primary components of fibres are cellulose, hemicelluloses, and lignin. The majority of cellulose is made up of crystalline and amorphous structures, while hemicellulose and lignin are amorphous[30]. The major crystalline peak of cellulose appears between 21.46° and 22.06° (002 plane), which indicates the crystallographic plane of

cellulose[31]. Amorphous peaks are observed between 18.32° and 18.58° (I_{am}) within the range of 0 0 2 to 1 0 1[32]. Removal of non-cellulosic materials such as hemicellulose and lignin through alkali treatment increases the crystallinity index by enabling stronger hydrogen bonding within cellulose chains[33]. As shown in Table 5, untreated fibres exhibit a crystallinity index of 63.51 %, which increases to 66.30 % after alkali treatment. GO-coated fibres show a slightly reduced crystallinity (65.92 %) owing to the amorphous nature of graphene oxide, while rGO-coated fibres reach the highest crystallinity index (68.41 %), reflecting improved ordering of cellulose microfibrils. These findings confirm that rGO enhances fibre crystallinity and ordering more effectively than GO.

3.3 FTIR Analysis

The FTIR spectra (Fig. 4) provide further confirmation of structural modifications in sisal fibres under different treatments. It shows a broad absorption band at 3600-3000 cm^{-1} with peak intensity at 3270 cm^{-1} for sisal fibres, corresponding to OH stretching vibrations in cellulose and hemicellulose. The intensity of this band increases after alkali treatment and GO coating, indicating enhanced hydroxyl interactions. The CH stretching peak at 2920 cm^{-1} decreases after GO/rGO coating, while the C=O peak at 2354 cm^{-1} intensifies, confirming successful graphene incorporation. The peak at 2850 cm^{-1} represents the vibration of the symmetrical elongation of the C-H bond between the CH_2 and CH groups of cellulose and hemicelluloses[34]. The peak at 1731cm^{-1} is attributed to the carboxylic ester (C = O) bond in lignin and wax, which reduces after alkali treatment[35] followed by GO and rGO coating. An intense peak at 1605 cm^{-1} is determined by the C = C stretching vibration[36] due to the phase combination of cellulose. The peak at 1425 cm^{-1} is attributed to C = C stretch and CH_2 symmetric bending in lignin, hemicelluloses and pectin[2]. Peaks at 1315 cm^{-1} show C = O stretching[37]. The peak at 1242 cm^{-1} shows the C - H bond[38]. The stretching of C - C bond in cellulose is associated with the 1013 cm^{-1} band[39]. The peak at 760 cm^{-1} is assigned to the CH_2 vibration in cellulose. Collectively, the FTIR results confirm that GO and rGO coatings are successfully deposited on fibre surfaces and actively modify surface chemistry.

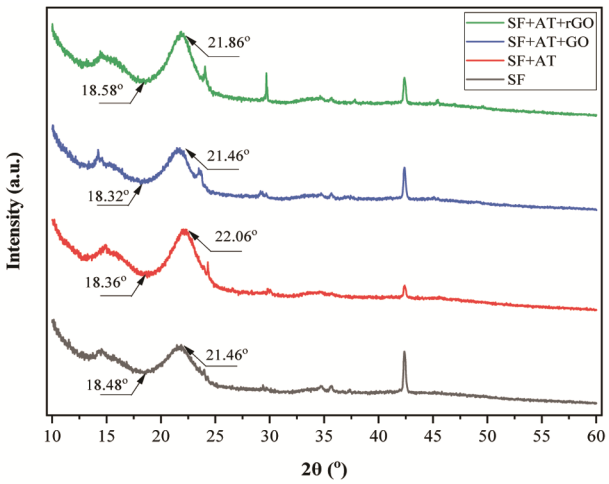

Fig. 3 — XRD patterns of untreated, alkali-treated, GO-coated, and rGO-coated sisal fibres

3.4 SEM

SEM images (Fig. 5) show significant variations in fibre surface morphology. Untreated fibres (Fig. 5 (a)) display relatively smooth surfaces due to the presence of waxes, lignin, and impurities. Alkali treatment eliminates much of this material, producing a rougher surface with improved fibre–matrix compatibility (Fig. 5 (b)). The deposition of GO and rGO on alkali-treated fibres produces thin, uniform coatings, confirming successful surface modification [Figs 5 (c) and (d)].

Fractured fibre surfaces [Fig. 5 (e) – (h)] further reveal that untreated fibres fail unevenly due to microfibril slippage. In contrast, GO- and rGO-coated fibres exhibit more compact structures and cleaner fracture surfaces, with GO/rGO filling microfibril voids and enhancing bonding. This microstructural improvement is consistent with the observed increases in tensile strength and interfacial shear strength.

Table 5 — Crystallinity index of sisal fibres under various treatments

	2θ, °		Intensity, a.u.			
Sample	I_{am}	I_{002}	$I8_{am}$	I_{002}	Crystallinity index, %	Percentage of crystallinity
SF	18.48	21.46	148.23	258	42.54	63.51
SF+AT	18.36	22.06	176.47	347.33	49.19	66.30
SF+AT+GO	18.32	21.46	139.33	269.61	48.32	65.92
SF+AT+rGO	18.58	21.86	164.82	357.04	53.83	68.41

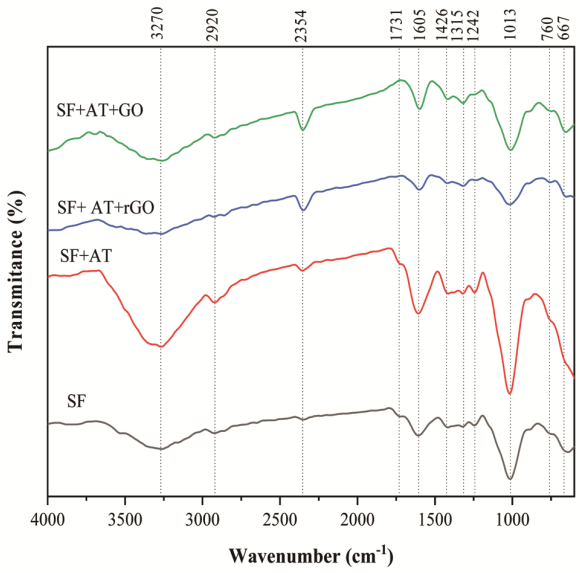

Fig. 4 — FTIR spectra of untreated, alkali-treated, GO-coated, and rGO-coated sisal fibres

3.5 Tensile Properties

The tensile behaviour of untreated, treated, and coated fibres is shown in Fig. 6 and summarised in Table 6. Untreated sisal fibres exhibit tensile strength and modulus values of 270.45 MPa and 4.53 GPa, respectively. The tensile strength and Young's modulus of sisal fibres treated with NaOH are increased by 22 % (to 4.53 GPa) and 44 % (to 270.45 MPa), respectively. Although tensile strength and modulus both increase after alkali treatment, extension at the break and breaking force decrease by 10 % and 20 %, respectively. This might be due to voids caused by unequal elimination of contaminants from the fibre surface using alkali treatment[14]. Previous research shows that the tensile strength of natural fibres is mainly dependent on the diameter of the fibres and the cellulose content present in them. The intense bleaching action of NaOH (alkali) solution eliminates contaminants from the fibre's surface. The bleaching action also eliminates lignin from the intercellular area of sisal fibres. It breaks down hemicellulose from the interfibrillar region, causing the fibres to separate from the cell and shrink in diameter[40]. A. Mukherjee *et al.*[40] reported that the decrease in extension at rupture and breaking force of the natural fibre may be caused by eliminating a substantial proportion of lignin. In addition, due to the elimination of lignin, natural fibres' intercells may shear quickly at a smaller force and stretch during the application of tensile loading. Fig. 5 (e) shows the SEM image of the fractured surface of an

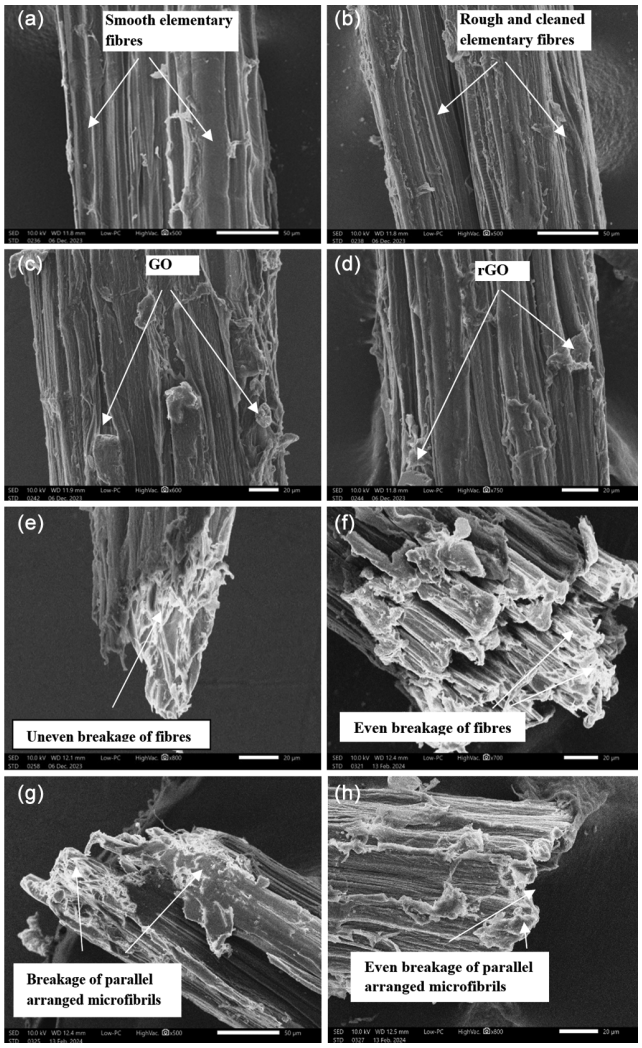

Fig. 5 — SEM images of (a) untreated (b) alkali-treated (c) GO-coated, and (d) rGO coated sisal fibres, along with SEM images of the fracture surfaces during tensile testing for (e) untreated, (f) alkali-treated, (g) GO-coated, and (h) rGO coated sisal fibres

untreated single sisal fibre. This image shows the broken surface of untreated single sisal fibres, which reveals an uneven breakdown because of the angular configuration of microfibrils. Baley *et al.*[41] have described the same chain of events in flax fibres, telling us that these microfibrils slip under a rough load because localised shear tension develops among them. Fig. 5 (f – h) displays the SEM images of the fractured surfaces of alkali-treated sisal fibre, as well as those treated with GO and rGO coatings. The SEM image of GO/rGO coated sisal fibre demonstrates that the holes of cellulose microfibrils are filled with GO/rGO, resulting in increased fibre compaction and even fibres breaking [Fig. 5(g -h)], hence producing enhanced tensile characteristics.

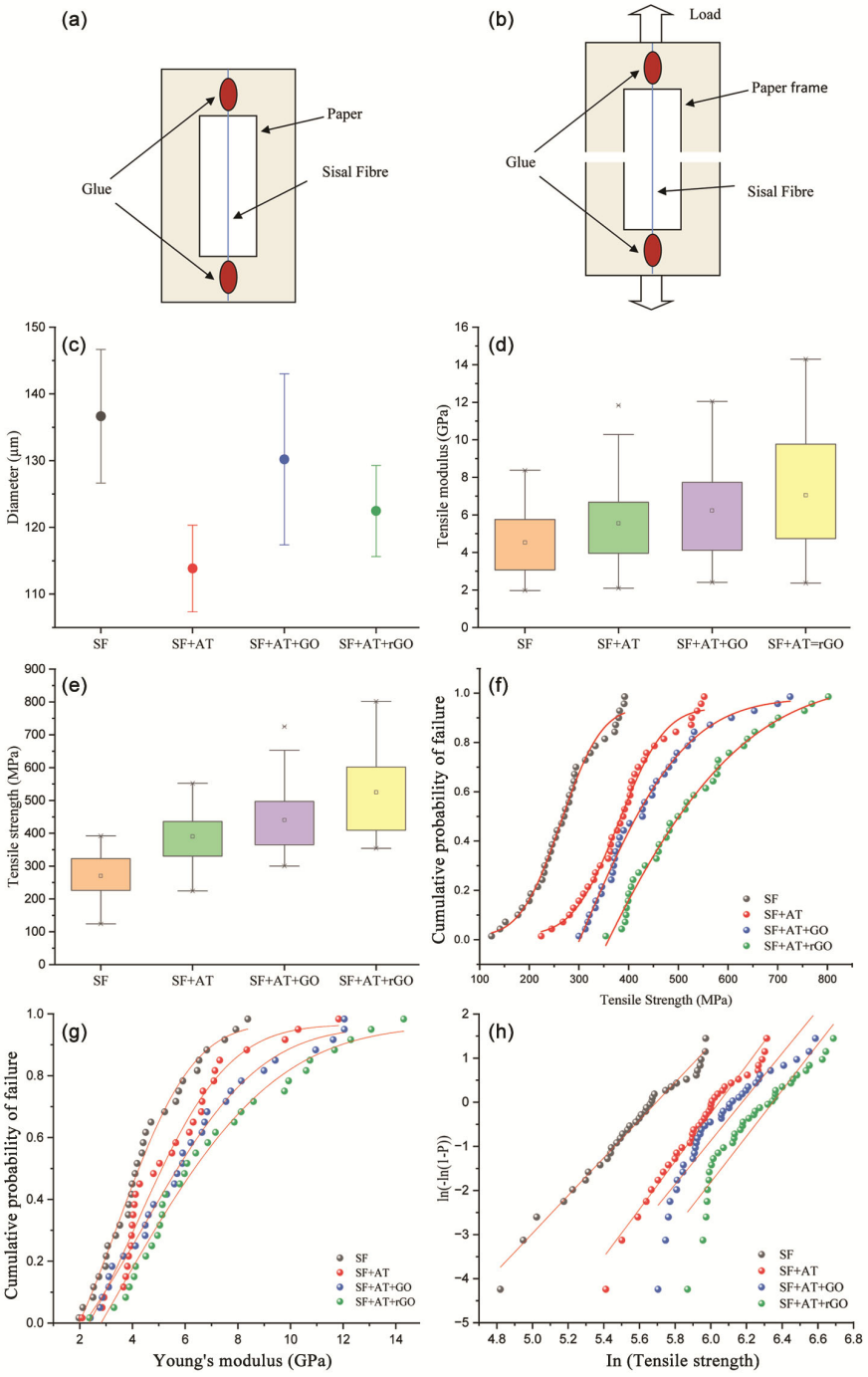

Fig. 6 — Mechanical characterisation: (a) paper card frame before tensile test, (b) paper card frame during tensile test, (c) fibre diameter, (d) tensile modulus, and (e) tensile strength of untreated, alkali-treated, GO-coated, and rGO-coated sisal fibres; (f) Weibull distribution of tensile strength, (g) Weibull distribution of Young's modulus as a function of surface treatment, and (h) ln curves of Weibull parameter plot distribution considering tensile strength

GO and rGO coatings further enhance mechanical properties, with tensile strength rising to 440.61 MPa (GO) and 524.91 MPa (rGO) and modulus to 6.23 GPa (GO) and 7.04 GPa (rGO) (Table 6). These represent increases of 62–94 % for tensile strength and 37–55 % for modulus compared to untreated fibres. The improvements are attributed to strong interfacial bonding between GO/rGO functional

Table 6 — Tensile properties of sisal fibres with statistical analysis

	Tensile strength, MPa				Tensile modulus, GPa			
	SF	SF+AT	SF+AT+GO	SF+AT+rGO	SF	SF+ AT	SF+AT+GO	SF+AT+rGO
Mean value	270.45	390.02	440.61	524.61	4.53	5.55	6.23	7.04
Standard deviation	72.83	86.52	109.82	121.66	1.74	2.31	2.85	3.17
Scale parameter, t_0	297.54	422.12	482.60	570.80	5.05	6.21	7.00	7.90
Shape parameter, m	4.27	5.42	4.94	5.20	3.13	2.97	2.61	2.68
Correlation, R^2	0.98	0.96	0.88	0.86	0.94	0.91	0.92	0.93

Table 7 — Interfacial properties of untreated and treated sisal fibres and its statistical analysis

	IFSS, MPa			
	SF	SF+AT	SF+AT+GO	SF+AT+rGO
No of samples tested	50	50	50	50
Mean value	1.95	2.80	3.83	4.48
Standard deviation	1.52	2.99	3.25	3.72
Scale parameter, t_0	2.14	3.13	4.28	4.89
Shape parameter, m	4.40	2.86	3.17	4.72
Correlation, R^2	0.95	0.94	0.88	0.96

groups and cellulose, coupled with the inherent stiffness of graphene derivatives. Weibull analysis (Fig. 6f–h) confirms these trends, with scale and shape parameters indicating improved fibre reliability after surface modification. The tensile strength of sisal fibres treated with NaOH and coated with GO and rGO is increased by 12 % and 34 %, respectively, and tensile modulus by 12 % and 26 %, respectively, compared to alkali-treated sisal fibres. Additionally, the extraordinarily high modulus of GO and rGO has the potential to stiffen sisal fibre and eliminate surface stress concentrations while tensile loading, improving the tensile properties of sisal fibre.

3.6 Interfacial Shear Strength

Interfacial shear strength **(**IFSS) is an important parameter used to evaluate the performance of FRP. A good interfacial bonding at the fibre/matrix contact is necessary to effectively transfer load from the matrix to the reinforcement. As a result, the composites' overall mechanical characteristics may be improved, and the stress concentration can be decreased. IFSS significantly influences several properties, such as fatigue life, fracture toughness, compressive strength, damage initiation threshold, and strain to failure.

The results from Table 7 and Fig. 7 show that both alkali treatment and GO/rGO coatings significantly improve the interfacial shear strength (IFSS) of sisal fibres. A microbond pull-out test is employed to measure IFSS between the fibre surface and matrix material Fig. 7 (a). The untreated fibres (SF) exhibit the weakest interfacial bonding (1.95 MPa) Fig. 7 (b), which can be attributed to the presence of surface impurities and waxy layers that restrict effective stress transfer at the fibre–matrix interface. After alkali treatment (SF+AT), the removal of hemicellulose, pectin, and lignin produces a rougher fibre surface (2.80 MPa), which promotes better adhesion with the epoxy matrix. Previous studies also reported that the IFSS value increased by alkali treatment of sisal and other natural fibre composites by 30-140 %. After coating graphene oxide and reduced graphene oxide onto sisal fibres that have undergone a 5 % alkali treatment, the single-fibre microbond test reveals a further appreciable increase in the value of IFSS.

The application of GO and rGO coatings further enhances the IFSS to 3.83 MPa and 4.56 MPa, respectively, compared with 1.95 MPa for untreated fibres. These values represent increases of approximately 95% and 133%, indicating the strong contribution of functionalised graphene layers toward fibre–matrix bonding. GO-coating increased the IFSS value of composite reinforced with synthetic fibres by 50–70 % in some earlier studies[42]. The presence of oxygen-containing functional groups in GO, as confirmed by FTIR (Fig. 4), facilitates chemical interactions, hydrogen bonding, and mechanical interlocking with the epoxy matrix. In the case of rGO-coated fibres, the partial reduction of oxygen functionalities enhances van der Waals interactions[43] and improves the stacking behaviour of graphene sheets, thereby providing additional reinforcement at the interface.

Moreover, the partial decrease of GO and the presence of epoxy LY556 polymers in rGO dispersions may cause the graphene sheets to stack and slide more, increasing their elongation and breaking force.

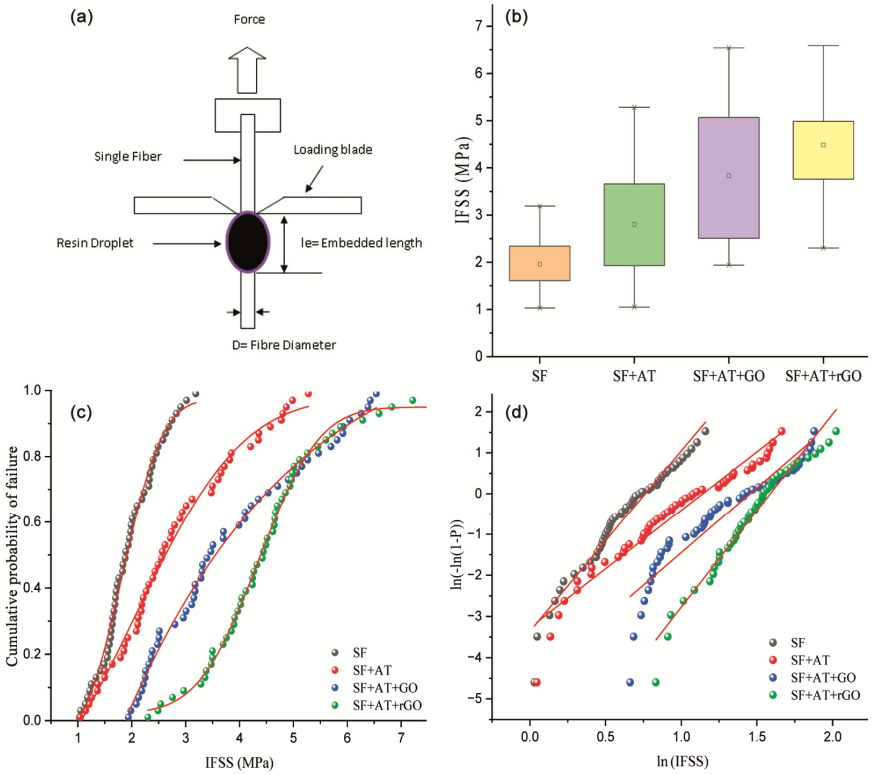

Fig. 7 — Interfacial characterisation: (a) schematic diagram of microbond testing, (b) IFSS of untreated, alkali-treated, GO-coated, and rGO-coated sisal fibres, (c) Weibull distribution of IFSS as a function of surface treatment, and (d) ln curves of Weibull parameter plot distribution considering IFSS

Additionally, the fibre/epoxy network is solidified using an amine-based hardener, which can create C-N linkages by ring-opening polymerisation[44]. Furthermore, because sisal fibres treated with 5 % NaOH have improved hydrophilicity, GO offers good adherence and homogeneous coating on the fibre's surface. Additionally, the layer of unwanted materials is removed from the sisal fibres after alkali treatment, creating a rough surface that is comparable to what was shown in the earlier study. Graphene oxide behaves like fillers on the rough surface between the cellulose chains of the fibres, generating powerful hydrogen bonds that improve the IFSS of 3.83 MPa between the matrix and fibres interface.

The statistical analysis using a two-parameter Weibull distribution (Table 7, Fig. 7c–d) provides further insights into interfacial performance. The scale parameter (τ_0) progressively increases from 2.14 MPa (untreated fibres) to 4.89 MPa (rGO-coated fibres), highlighting the increase in the characteristic IFSS strength. Meanwhile, the shape parameter (m), which indicates the variability in failure strength, is highest for rGO-coated fibres (4.72), suggesting a more uniform distribution of defects and enhanced reliability of the interfacial bonding. The lower Weibull modulus observed for untreated fibres confirms a higher probability of premature failure due to surface flaws.

4 Conclusion

This study demonstrates that coating sisal fibres with graphene oxide (GO) and reduced graphene oxide (rGO) using a dip-coating method significantly improves their structural and interfacial properties. The GO and rGO-coated fibres show enhancements in tensile strength by 62% and 94%, respectively, and in interfacial shear strength by 95% and 133%, compared with untreated fibres. Thermal, chemical, and microstructural characterisations (FTIR, TGA, XRD, and SEM) confirm that the functionalisation of sisal fibres after alkali treatment facilitates better fibre–matrix bonding and contributes to improved performance. FTIR spectra indicate the removal of lignin after alkali treatment and the presence of oxygen-rich functional groups in GO-coated fibres, while TGA and XRD reveal improvements in thermal

stability and crystallinity. The combined effect of alkali treatment and GO/rGO coatings produces high-performing fibres with enhanced mechanical, thermal, and interfacial properties, while maintaining environmental compatibility. Such fibres hold strong potential for use in advanced composite applications, including automotive interior components, aerospace structures, marine products, ropes and nets, and other engineering sectors requiring lightweight and sustainable reinforcement materials.

References

1 Hu C, Zhou Y, Zhang T, Jiang T & Zeng G, *J Reinf Plas Comp*, 39 (2020) 880.
2 Da Silveira P H P M, Ribeiro M P, Silva T T, Lima A. M, Lemos M F, Oliveira A G B A M, Nascimento L F C, Gomes A V & Monteiro S N, *J Nat Fibers*, 19 (2022) 12168
3 Kamarudin S H, Mohd Basri M S, Rayung M, Abu F, Ahmad S, Norizan M N, Osman S, Sarifuddin N, Desa M S Z M, Abdullah U H, Tawakkal I S M A & Abdullah L C, *Polym*, 14 (2022) 3698.
4 Armanfard A & Melenka G W, *Compo Struct*, 269 (2021) 114049.
5 Hakim A A & Mourad R M, *Polym Compos*, 41 (2019) 1435.
6 Alvarez V A, Ruscekaite R A & Vazquez A, *J Compos Mater*, 37 (2003) 1575.
7 Jayapalan S, *J Innov Soc Sci Res*, 9 (2022).
8 Nurazzi N M, Khalina A, Sapuan S M, Ilyas R A, Rafiqah S A & Hanafee Z M, *J Mater Res Technol*, 9 (2020) 1606.
9 Bekele A E, Lemu H G & Jiru M G*, Polym Test*, 106 (2022) 107453
10 Chand N & Joshi R, *J Nat Fibers*, 7 (2010) 100.
11 Hakim A A & Mourad RM, *Polym Compos*, 41 (2019) 1435.
12 Hu C, Zhou Y & Zeng G, 39 (2020)
13 Sahu P & Gupta M K, *Polym Test*, 93 (2021) 106923.
14 Behra S, Gautam R K & Mohan S, *Cellulose*, 29 (2022) 9055.
15 Jena S, Khatri V N, Nainegali L & Dutta R K, *Fibres Polym*, 25 (2024) 2517.
16 Zhao L, Zhu S, Wu H, Liang H, Liu C, Liu W, Zhou W & Song Y, *Constr Build Mater*, 305 (2021) 124694.
17 Sarker, Potluri P, Afroj S, Koncherry V, Novoselov K S & Karim N, *ACS Appl Mater Interfaces*, 11 (2019) 21166.
18 Colusso E & Martucci A, *J Mater Chem C*, 9 (2021) 5578.
19 Sarker F, Karim N, Afroj S, Koncherry V, Novoselov K S & Potluri P, *A C S Appl Mater Interfaces*, 10 (2018) 34502.
20 Hallad S A, Banapurmath N R, Patil V, Ajarekar V S, Patil A, Godi M T & Shettar A S, *I O P Conf Ser Mater Sci Eng*, 276 (2012) 012072.
21 Costa U O, Nascimento L F C, Garcia J M, Monteiro S N, Luz F S D, Pinheiro W A & Filho F D C G, *Polym*, 11 (2019) 1356.
22 Filho F D C G, Luz F S D, Oliveira M S, Pereira A C, Costa U O & Monteiro S N, *J Mater Res Technol*, 9 (2020) 5343.
23 Silveira P H P M D, Ribeiro M P, Silva T T, Lima A M, Lemos M F & Oliveira A G B M, *J Nat Fibers*, 19 (2022) 12168.
24 Sahu P & Gupta M K, *I O P Conf Ser Mater Sci Eng*, 455 (2018) 012014.
25 https://ad-nanotech.com/graphene-oxide-2/ (dt: 15/08/2024)
26 Segal L, Creely J J, Martin A E & Conrad C M, *Text Res J*, .29 (1959) 786.
27 Silva T, Silveira P, Ribeiro M, Lemos M, Da Silva A, Monteiro S & Nascimento L, *Polym*, 13 (2021) 2016.
28 Ayalew A A & Wodag A F, *J Eng*, 2022 (2022)
29 Kandola B, Sarker F & Luangtriratana P, P Myler, *Coating*, 6 (2016) 22.
30 Rahman N H A, Chieng B W, Ibrahim N A & Rahman N A, *Polym*, 9 (2017) 588.
31 Boudjellal A, Trache D, Khimeche K, Hafsaoui S L & Razali M S, *J Nat Fibers*, 19 (2021) 5321.
32 Park S, Baker J O, Himmel M E, Parilla P A & Johnson D K, *Biotechnol Biofuels*, 3 (2010).
33 Mbeche S M & Omara T, *Peer J Mater Sci*, 2 (2020) 5.
34 Zhang H, Ming R, Yang G, Li Y, Li Q & Shao H, *Polym Eng Sci*, 55 (2015) 2553.
35 Dai D & Fan M, *Mater Sci Appl*, 01 (2010) 336.
36 Berra D, Laouinia S E, Benhaoua B, Ouahrani M R, Berrani D & Rahal A, *Digest J Nanomater Biostruct*, 13 (2018) 1231
37 Yuen S N, Choi S M, Phillips D L & Ma C Y, *Food Chem*, 114 (2009) 1091.
38 Pimentel M G P, Ramirez N F, Sanchez J C F, Lvova L D, Garcia S N R V & Gonzalez L G, *Superf Vacío,* 3 (2016) 29
39 Thomas S K, Begum P M S, Dileep P, Neenu K V, David D A, Santu A & Dominic C D M, *Biomass Convers Biorefinery*, (2023).
40 Mukherjee A, Ganguly P K & Sur D, *J Text Inst*, 84 (1993) 348.
41 Doan T T L, Brodowsky H & Mäder E, *Compos Sci Technol*, 72 (2012) 1160.
42 Chen L, Wei F, Liu L, Cheng W, Hu Z, Wu G, Du Y, Zhang C & Huang Y, *Compos Sci Technol*, 106 (2015) 32.
43 Xu Z, Sun H, Zhao X & Gao C, *Adv Mater*, 25 (2012) 188.
44 Wang S, Chia P, Chua L, Zhao L, Png R, Sivaramakrishnan S, Zhou M, Goh R G S, Friend R H, Wee A T S & Ho P K H, *Adv Mater*, 20 (2008) 3440.